

The Molecular Docking of Specific Reverse Transcriptase Inhibitory Ligands onto the Molecular Model of HIV-1 Reverse Transcriptase

Roohallah Yousefi^{1,2*}; PhD 

¹Behbahan Faculty of Medical Sciences, Behbahan, Iran

²Department of Biochemistry, Faculty of Biological Sciences, Tarbiat Modares University, Tehran, Iran.

Abstract

HIV-1 reverse transcriptase (RT) is a crucial enzyme in HIV replication and AIDS progression. It consists of p66 and p51 subunits and converts viral RNA into double-stranded DNA for integration into the host cell's genome. Managing HIV/AIDS depends on inhibiting HIV-1 RT, achieved through nucleoside reverse transcriptase inhibitors (NRTIs) and non-nucleoside reverse transcriptase inhibitors (NNRTIs). Understanding RT's structure, catalysis, inhibition, and resistance has been vital for disease management. To study the binding sites and interactions of reverse transcriptase inhibitors (RTIs) with HIV-1 RT, we utilized Molegro Virtual Docker for model preparation and docking. We also employed the SwissADME web tool for predicting physicochemical properties and pharmacokinetics of compounds of interest. We investigated the binding site and affinity of antiretroviral drugs, including delavirdine, tenofovir alafenamide, and atavirdine, with the HIV-1 RT enzyme. Additionally, we evaluated factors such as gastrointestinal absorption, blood-brain barrier penetration, Pgp substrate status, and skin permeability to assess the efficacy of these drugs in treating HIV/AIDS. The findings of this study may help us understand the interactions and potential applications of these compounds with other drugs, ultimately improving antiretroviral therapy for managing HIV-1 infection. Understanding the binding affinity, sites, and pharmacological properties of reverse transcriptase inhibitor compounds is crucial for developing effective antiretroviral therapies against HIV/AIDS.

Keywords: HIV-1, Reverse Transcriptase (RT), p66 and p51 subunits

Please cite this article as: Yousefi R*. The molecular docking of specific reverse transcriptase inhibitory ligands onto the molecular model of HIV-1 reverse transcriptase. Trends in Pharmaceutical Sciences. 2024;10(2):91-112. doi: 10.30476/TIPS.2024.102488.1239

1. Introduction

The global HIV epidemic continues to impact millions of lives, with approximately 39 million people living with the virus, including 37.5 million adults and 1.5 million children under the age of 14 as of 2022 (1, 2).

HIV-1 reverse transcriptase (RT) is a crucial enzyme in the replication of the Human Immunodeficiency Virus (HIV) and plays a significant role in the progression of Acquired Immunodeficiency Syndrome (AIDS). RT is responsible for

converting the viral RNA genome into a double-stranded linear DNA, which can then be integrated into the host cell's genome by the viral enzyme integrase (IN) (3, 4).

The DNA polymerase activity of reverse transcriptase (RT) allows it to copy both DNA and RNA templates, synthesizing new DNA strands that are complementary to the templates. In the case of HIV, RT uses a host tRNA molecule as a primer and the viral RNA genome as the template. This process involves two stages: first-strand synthesis and second-strand synthesis. During first-strand synthesis, RT generates a positive-sense, full-length cDNA copy of the viral RNA genome, known as the strong-stop DNA. In the second-

Corresponding Author: Roohallah Yousefi, Department of Biochemistry, Faculty of Biological Sciences, Tarbiat Modares University, Tehran, Iran
Email: ry@behums.ac.ir

strand synthesis, the enzyme synthesizes the complementary negative-sense DNA strand, resulting in a double-stranded linear DNA molecule called the proviral DNA. The RNase H activity of RT is responsible for cleaving the RNA component from the RNA/DNA hybrid molecules formed during the reverse transcription process (3-5).

1.1. The Structure of the HIV-1 RT Enzyme

The HIV-1 RT enzyme is an asymmetric heterodimer composed of two subunits: p66 and p51. The p66 subunit contains the active sites for both DNA polymerase and RNase H activities, while the p51 subunit plays a structural role and shares the polymerase domain with p66. Additionally, the p66 subunit contains a unique domain called the connection domain, which is involved in the interaction between the two subunits. HIV-1 reverse transcriptase was the first drug target in the treatment of AIDS. Both nucleoside and non-nucleoside reverse transcriptase inhibitors are essential components of highly active antiretroviral therapy (HAART) (6, 7).

Efavirenz and other NNRTIs are a class of small amphiphilic compounds that bind to RT and inhibit viral replication. The biologically active form of RT is an asymmetric heterodimer composed of 66 and 51 kDa subunits. The p66 subunit contains polymerase and RNase H domains. The polymerase domain consists of four subdomains: fingers (1–85, 118–155 amino acids), palm (86–117, 156–236 amino acids), thumb (237–318 amino acids), and connection (319–426 amino acids). The p51 subunit comprises the polymerase domain of p66 with a different tertiary fold of the four subdomains. Both the DNA polymerase and RNase H active sites are located in the p66 subunit. In virus-infected cells, the p66 subunit is expressed as part of the 160 kDa Gag-Pol polyprotein, which is subsequently processed by the encoded HIV-1 protease. The mechanism of maturation of the RT heterodimer is not fully understood. Two models have been proposed. In the concerted model, p66 and p51 monomers are derived from separate Gag-Pol precursor peptides. In contrast, the sequential model suggests that the p51 subunit is generated from the p66 subunit through proteolytic cleavage (6-9).

1.2. HIV-1 Reverse Transcriptase (RT) Inhibition

Inhibiting HIV-1 reverse transcriptase (RT) is a crucial aspect of fighting against HIV, as it targets the enzyme responsible for converting the viral RNA genome into double-stranded linear DNA that can integrate into the host genome. This integration is essential for the virus's replication and persistence within the host. To effectively combat HIV, researchers have developed two primary classes of antiretroviral drugs: nucleoside reverse transcriptase inhibitors (NRTIs) and non-nucleoside reverse transcriptase inhibitors (NNRTIs). NRTIs function as chain terminators, inhibiting RT by incorporating themselves into the growing viral DNA chain, preventing further DNA synthesis. These drugs must be converted into their active form by cellular enzymes before they can inhibit RT. Novel NRTIs, such as 4'-ethynyl-2-fluoro-2'-deoxyadenosine (EFdA), have emerged with alternative mechanisms and higher resistance to drug resistance. EFdA acts as an immediate or delayed chain terminator (ICT or DCT) due to its 3'-OH group and tight binding to RT, causing structural distortions and misincorporation (10, 11).

Entecavir (ETV), an FDA-approved drug for hepatitis B virus (HBV), acts as a delayed chain terminator (DCT). Although HBV RT structures were used as surrogates due to their intractability, this approach provided insights into ETV's binding specificity differences between HIV-1 and HBV RT. Understanding NRTIs' mechanisms, resistance, and potential for novel stereochemistry NRTIs is crucial for developing more effective and long-acting antiretroviral therapies against HIV/AIDS. Non-nucleoside reverse transcriptase inhibitors (NNRTIs) work by binding to a specific pocket adjacent to the polymerase active site of RT, causing structural rearrangements that interfere with the chemical step of DNA synthesis. These drugs do not directly incorporate into the viral DNA. NNRTIs face resistance through mutations that disrupt specific contacts, alter important interactions, or change the overall conformation of the binding pocket. Examples include K103N, Y181C, and G190E mutation (10-13).

1.3. Non-nucleoside reverse transcriptase inhibitors (NNRTIs)

NNRTIs are a class of antiretroviral drugs used in the treatment of HIV. They work by binding to the reverse transcriptase enzyme, prevent-

ing the conversion of viral RNA into DNA, which is essential for the virus to replicate. Examples of NNRTIs include efavirenz, nevirapine, etravirine, and rilpivirine. NNRTIs have several advantages over other antiretroviral drugs. They have a higher genetic barrier to resistance, meaning it takes longer for the virus to develop resistance to them compared to other classes of antiretroviral drugs. However, NNRTIs also have limitations. They can interact with other medications, as they are metabolized by the same enzymes in the liver. This can lead to increased or decreased concentrations of the NNRTI or other drugs, potentially causing side effects or reduced efficacy. NNRTIs are usually combined with other antiretroviral drugs to form a combination therapy. This approach maximizes the effectiveness of the treatment and minimizes the risk of resistance development (14-18).

We examined the physicochemical and pharmacodynamic properties of 62 inhibitory ligands for the enzyme reverse transcriptase. In the present study on the enzyme reverse transcriptase model [PDB: 5TXM], we analyzed the docking results of binding of each ligand with the reverse transcriptase model.

2. Material and methods

2.1. Preparation of Reverse Transcriptase Model

The molecular model of reverse transcriptase [PDB: 5TXM] was obtained from the RCSB PDB database. The 5TXM model represents a ternary complex of HIV-1 reverse transcriptase (RT) in association with double-stranded DNA and an incoming ddATP. This essential structure, classified as a transferase/DNA complex, originates from Human Immunodeficiency Virus type 1 BH10 and Human Immunodeficiency Virus 1. The expression system used for this structure determination was *Escherichia coli*. We utilized parts of the model that included subunits P66 and P51 for docking (19).

2.2. Preparation of Ligand Model

To prepare ligand models for further analysis, 62 compounds consisting of non-nucleotide reverse transcriptase inhibitors were collected from the PubChem database (Figure 1A, 1B). Subsequently, the Molegro Virtual Docker tool, known for its effectiveness in ligand preparation, was employed for this purpose (20, 21).

2.3. Predicting Physicochemical Properties and Pharmacokinetics

To predict the physicochemical properties and pharmacokinetics of the compounds of interest in our study, we utilized the SwissADME web tool. This user-friendly platform, accessible at <http://www.swissadme.ch>, offers a range of quick and reliable predictive models, such as the BOILED-Egg, iLOGP, and others, to assess important drug development parameters. By employing SwissADME, we were able to efficiently evaluate the required properties (22-27).

2.4. Molecular Docking

We utilized Molegro Virtual Docker (MVD), a versatile and reliable software for molecular docking. This powerful tool predicts the binding affinity and orientation of small molecules to target proteins using advanced computational methods. MVD stands out for its flexible docking algorithm, which considers multiple conformations of both ligand and receptor molecules, ensuring accurate results in both rigid and flexible docking scenarios. Some notable features of MVD include grid-based scoring functions, support for multiple docking engines, and comprehensive output analysis tools, which aid in further exploration of docking results. With 32 docking protocols and the ability to consider the presence or absence of water molecules, MVD offers a robust platform for molecular docking analysis (21).

3. Results

3.1. Molecular Docking Results of Studied Compounds with Reverse Transcriptase

This study focused on the highest binding energy and corresponding binding sites of the ligands examined for the reverse transcriptase enzyme model. The binding sites for Delavirdine, Tenofovir Alafenamide, and Ateviridine in the HIV-1 reverse transcriptase (RT) enzyme involve specific residues distributed across both the p66 and p51 subunits of the enzyme, which are crucial for the interaction between the drugs and the enzyme.

For Delavirdine, the binding site in the p51 subunit includes Trp266, Ile270, Glu328, Ile329, Gln330, Lys331, Tyr342, Pro345, Phe346, Asn348, Pro392, Val417, Thr419, Pro420, Pro421, Val423, Leu425, and Trp426. In the p66 sub-

unit, the binding site consists of a single residue, Trp406.

In the case of Tenofovir Alafenamide, the primary binding site in HIV-1 RT involves residues in the p51 subunit, including Arg78, Asn81, Lys82, Glu85, Trp88, Glu89, K154, Tyr183, Asp324, Leu325, Gly384, Lys385, Thr386, Pro387, Lys388, Trp410, Ile411, Pro412, and Glu413.

The binding site for Ateviridine in HIV-1 RT consists of essential residues in both the p66 and p51 subunits. In the p51 subunit, these residues are Trp266, Gln330, Pro392, Val417, Asn418, Thr419, Pro420, Pro421, Leu422, Val423, Leu425, and Trp426. In the p66 subunit, the binding site comprises Trp406, Gln407, Gln500, and Trp535. Compounds with CID Numbers 5625, 60848, and

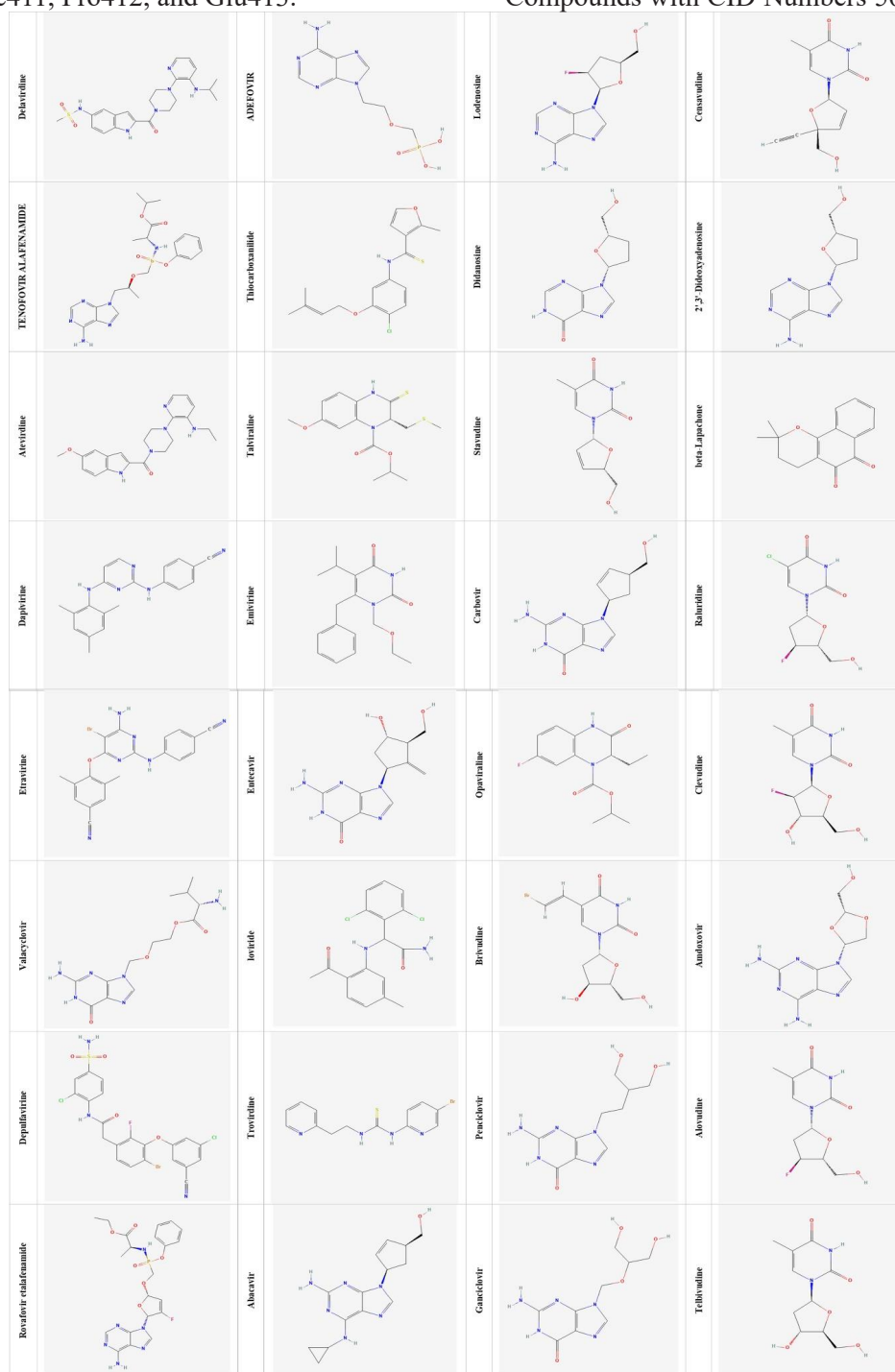


Figure 1A. 2D- structure of studied ligands

193962 have similar binding sites on amino acids Glu328, Ile329, Gln330, Lys331, Trp342, Pro345, Phe346, Asn348, Pro392, Val417, Thr419, Pro421, Leu422, Val423, Leu425, and Trp426 in the p51 subunit, including Trp406 in the p66 subunit.

Other compounds with CID numbers 73115, 3885, 20039, 3008897, 469717, 3963, 441300, 135398513, 53370, 72180, 135398739,

11599486, 451164, 73505111, 0172, 135398508, 214347, and 9574768 have similar binding sites involving amino acids Leu74, Val75, Asp76, Phe77, Arg78, Asn81, Lys82, Gln85, Trp88, Gln89, Gly93, Ile94, His96, Gly152, K154, Gly155, Pro157, Ala158, Tyr181, Q182, Tyr183, Met184, Ser322, Asp324, Leu325, Gly384, Lys385, Thr386, Pro387, Lys388, Thr409, Trp410,

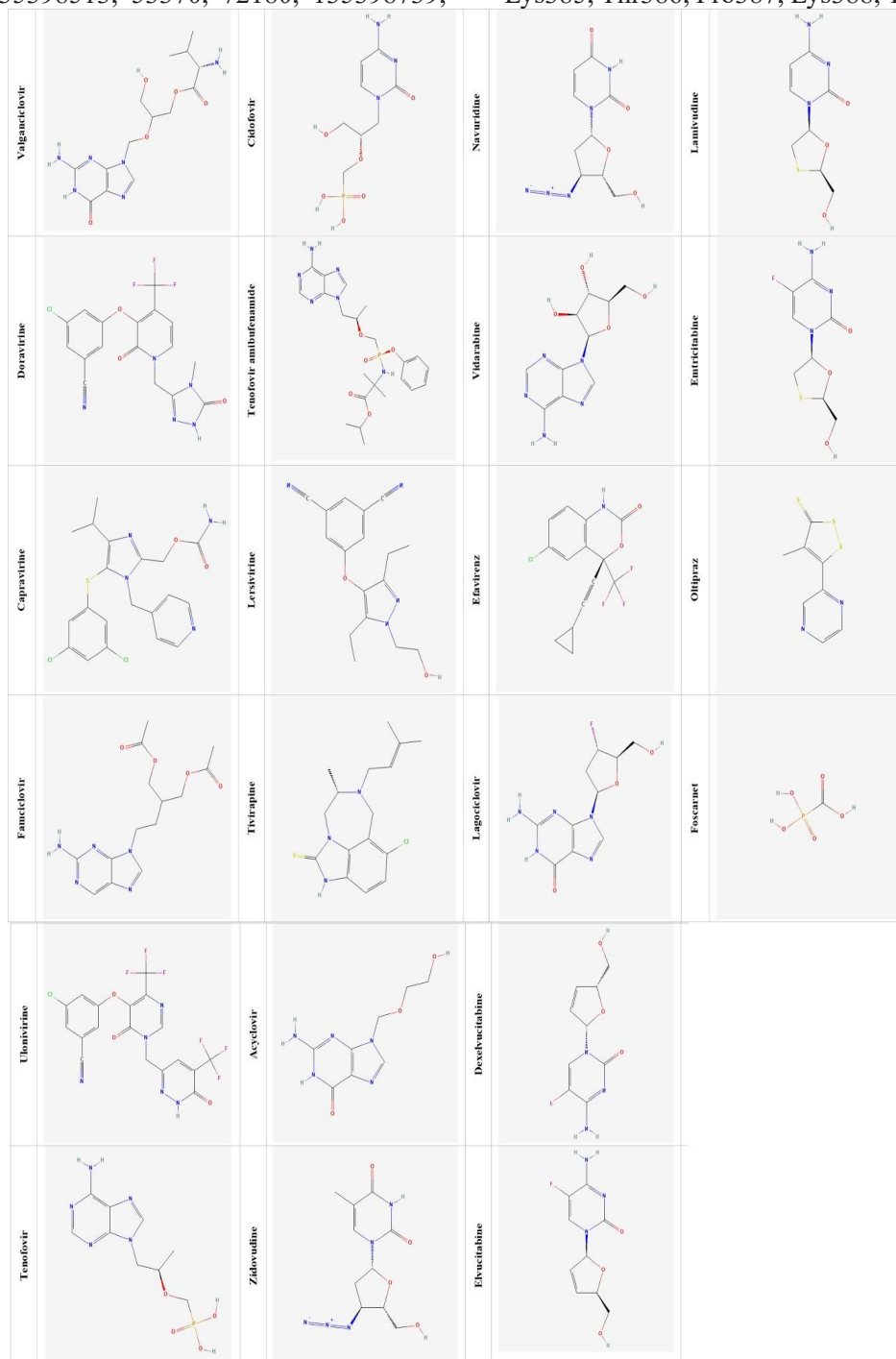


Figure 1B. 2D structure of the studied ligands.

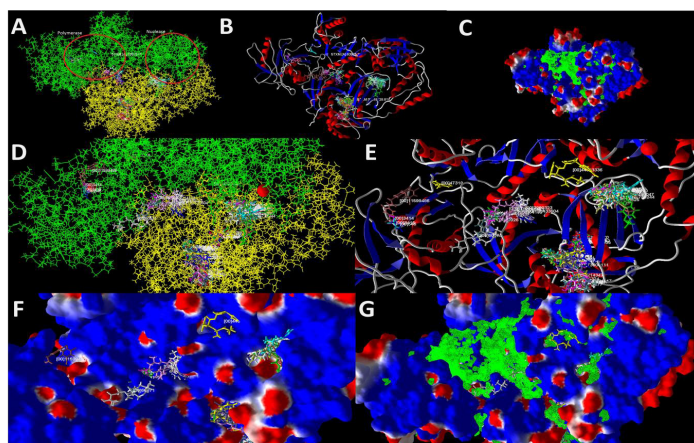


Figure 2. Representation of the reverse transcriptase enzyme model [PDB: 5TXM]. A: The wireframe model of the HIV-1 reverse transcriptase enzyme shows the active sites of the enzyme with polymerase and nuclease functions, The P66 sub-unit is shown in green, and the P51 sub-unit is shown in yellow. B: Secondary structure model of the HIV-1 reverse transcriptase enzyme. C: Model of the electrostatic surfaces of the HIV-1 reverse transcriptase enzyme. D: Wireframe model of the HIV-1 reverse transcriptase enzyme at higher magnification, showing ligand binding sites. E: Secondary structure of the HIV-1 reverse transcriptase enzyme at higher magnification, showing ligand binding sites. F: Higher magnification model of the HIV-1 reverse transcriptase electrostatic surfaces, showing ligand binding sites. G: Model of the electrostatic surfaces of the HIV-1 reverse transcriptase enzyme at higher magnification, showing the holes in the enzyme model.

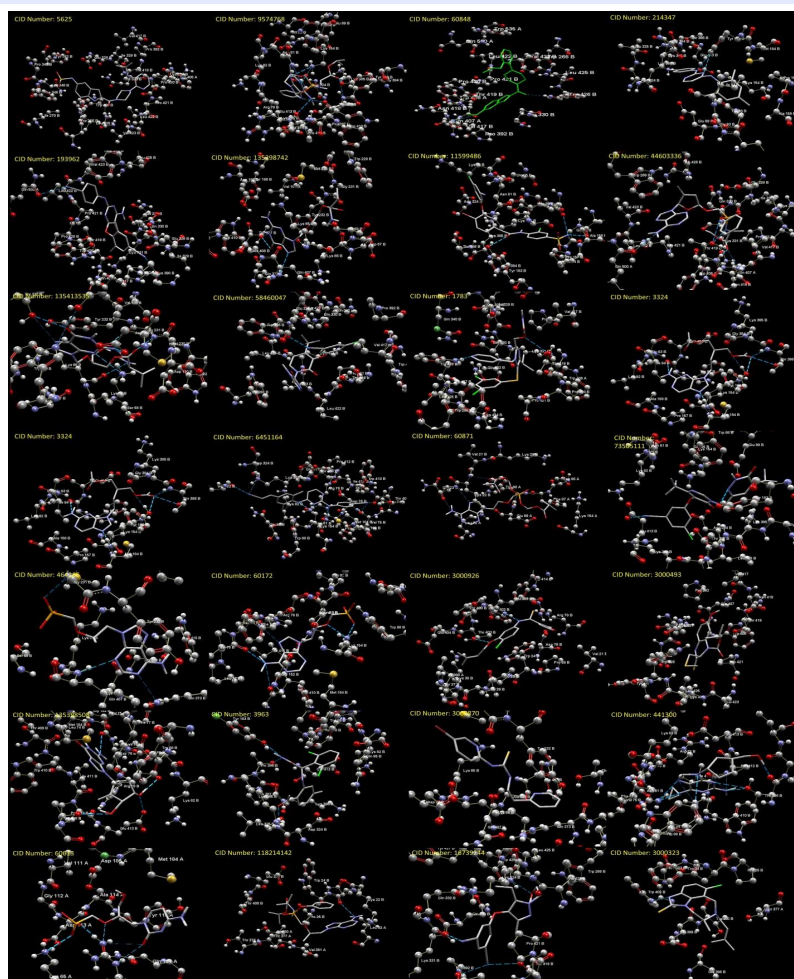


Figure 3A. The binding site of 28 of the studied compounds, in each image, A represents the p66 subunit, while B represents the p51 subunit. Hydrogen bonds are depicted as blue dashes, with their size corresponding to the bond energy.

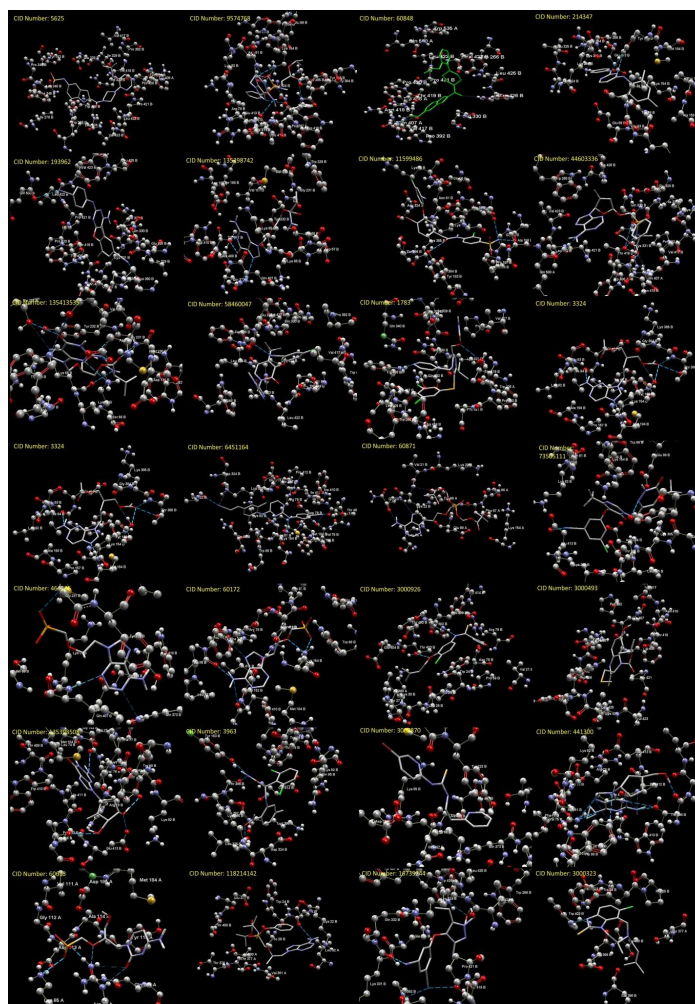


Figure 3B. The binding site of the remaining 38 studied compounds, in each image, A represents the p66 subunit, while B represents the p51 subunit. Hydrogen bonds are depicted as blue dashes, with their size corresponding to the bond energy.

Pro412, and Glu413 in the p51 subunit. The remaining compounds studied have binding sites in both the p51 and p66 subunits. Figure 2 shows the molecular model of the enzyme and the binding sites of the ligands, while Figures 3A and 3B show the hydrogen bonds formed between the functional groups of amino acids in the binding site and the functional groups on the ligand. Table 1 shows the highest binding affinity for each compound on the reverse transcriptase model.

3.2. Physicochemical properties of studied compounds

Molecular weight is an important and effective indicator of physicochemical properties. Compounds with a weight above 500 Daltons have limited digestive absorption. The heaviest compound in our study, Depulfavirine, has a weight of 573.22 Daltons. This compound has a lower ligand efficiency ($LE1 = \text{MolDock Score} / \text{Heavy Atoms}$)

than most of the studied compounds. Additionally, it is weakly hydrophobic and does not dissolve well in physiological fluids, leading to poor digestive and skin absorption. Adefovir dipivoxil, with CID number 60871 and a molecular weight of 501 Daltons, has good solubility but very poor digestive absorption. This compound strongly inhibits liver cytochrome P450 enzymes. Compounds with a molecular weight less than 500 Daltons often have good solubility in physiological body fluids and good digestive absorption. Only compounds with CID numbers 9574768, 60848, 193962, 1783, 60871, 3000926, 3000493, 118214142, and 3000323 have iLOGP over 3.1, but all of these compounds are in the range of very soluble to moderately soluble (Table 2).

3.3. Pharmaceutical Properties of studied compounds

Most of the studied ligands have good

Table 1. Molecular docking results of studied compounds with Reverse Transcriptase model [PDB: 5TXM].

CID Numbers	Name	IUPAC Name	Interaction	MolDock Score	LE1	Torsions	HBond	Heavy Atoms	MW
5625	Delavirdine	N-[2-[4-[3-(propan-2-ylamino)pyridin-2-yl]piperazine-1-carbonyl]-1H-indol-5-yl]methanesulfonamide	-172.234	-147.591	-4.61223	5	-1.01068	32	453.537
9574768	TENOFOVIR ALAF-ENAMIDE	propan-2-yl (2S)-2-[[[(2R)-1-(6-aminopurin-9-yl)propan-2-yl]oxymethylphenoxyphosphoryl]amino]propanoate	-162.909	-145.691	-4.41487	12	-8.35627	33	476.466
60848	Ateviridine	[4-[3-(ethylamino)pyridin-2-yl]piperazin-1-yl]-(5-methoxy-1H-indol-2-yl)methanone	-161.353	-138.797	-4.95702	5	-2.29626	28	377.44
214347	Dapivirine	4-[[4-(2,4,6-trimethylamino)pyrimidin-2-yl]amino]benzotrile	-157.416	-129.333	-5.17331	5	-3.54524	25	327.382
193962	Etravirine	4-[6-amino-5-bromo-2-(4-cyanoanilino)pyrimidin-4-yl]oxy-3,5-dimethylbenzotrile	-157.304	-132.862	-4.74508	6	0	28	434.269
135398742	Valacyclovir	2-[(2-amino-6-oxo-1H-purin-9-yl)methoxy]ethyl (2S)-2-amino-3-methylbutanoate	-156.885	-154.127	-6.70115	8	-2.57355	23	324.336
11599486	Depufavirine	2-[4-bromo-3-(3-chloro-5-cyanophenoxy)-2-fluorophenyl]-N-(2-chloro-4-sulfamoylphenyl)acetamide	-154.994	-129.065	-3.91106	6	-2.77007	33	572.211
44603336	Rovafovir etalafenamide	ethyl (2S)-2-[[[(2R,5R)-5-(6-aminopurin-9-yl)-4-fluoro-2,5-dihydrofuran-2-yl]oxymethyl-phenoxyphosphoryl]amino]propanoate	-153.899	-153.61	-4.38885	11	-3.36809	35	505.416
135413535	Valganciclovir	[2-[(2-amino-6-oxo-1H-purin-9-yl)methoxy]-3-hydroxypropyl] (2S)-2-amino-3-methylbutanoate	-153.872	-138.617	-5.54467	9	-7.70479	25	354.362
58460047	Doravirine	3-chloro-5-[1-[(4-methyl-5-oxo-1H-1,2,4-triazol-3-yl)methyl]-2-oxo-4-(trifluoromethyl)pyridin-3-yl]oxybenzotrile	-153.141	-138.885	-4.78913	6	0	29	424.741
1783	Capravirine	[5-(3,5-dichlorophenyl)sulfanyl-4-propan-2-yl-1-(pyridin-4-ylmethyl)imidazol-2-yl]methyl carbamate	-152.875	-165.549	-5.70858	8	-2.5	29	451.369

Continued Table 1.

3324	Famciclovir	[2-(acetyloxymethyl)-4-(2-aminopurin-9-yl)butyl] acetate	-152.615	-143.157	-6.2242	9	-8.21005	23	321.332
6451164	Rilpivirine	4-[[4-[4-[(E)-2-cyanoethenyl]-2,6-dimethylanilino]pyrimidin-2-yl]amino]benzotrile	-152.446	-125.542	-4.48364	7	-2.8729	28	364.403
60871	ADEFOVIR DIPIVOXIL	[2-(6-aminopurin-9-yl)ethoxymethyl-(2,2-dimethylpropanoyloxymethoxy)phosphoryl]oxymethyl 2,2-dimethylpropanoate	-152.368	-126.027	-3.70667	15	-3.03379	34	501.471
73505111	Ulonivirine	3-chloro-5-[6-oxo-1-[[6-oxo-5-(trifluoromethyl)-1H-pyridazin-3-yl]methyl]-4-(trifluoromethyl)pyrimidin-5-yl]oxybenzotrile	-148.474	-106.768	-3.23538	7	-2.60377	33	491.731
464205	Tenofovir	[(2R)-1-(6-aminopurin-9-yl)propan-2-yl]oxymethylphosphonic acid	-139.587	-125.719	-6.61676	5	-3.67786	19	285.196
60172	ADEFOVIR	2-(6-aminopurin-9-yl)ethoxymethylphosphonic acid	-136.907	-134.698	-7.48323	5	-5.39197	18	271.17
3000926	Thiocarboxanilide	N-[4-chloro-3-(3-methylbut-2-enoxy)phenyl]-2-methylfuran-3-carbothioamide	-135.819	-120.753	-5.48879	5	-2.5	22	334.84
3000493	Talviraline	propan-2-yl (2S)-7-methoxy-2-(methylsulfanylmethyl)-3-sulfanylidene-2,4-dihydroquinoxaline-1-carboxylate	-135.779	-125.628	-5.71035	6	0	22	339.453
65013	Emivirine	6-benzyl-1-(ethoxymethyl)-5-propan-2-ylpyrimidine-2,4-dione	-133.049	-108.125	-4.91476	6	-2.94714	22	302.368
135398508	Entecavir	2-amino-9-[(1S,3R,4S)-4-hydroxy-3-(hydroxymethyl)-2-methylidenecyclopentyl]-1H-purin-6-one	-131.953	-129.463	-6.47315	2	-7.89473	20	277.279
3963	loviride	2-(2-acetyl-5-methylanilino)-2-(2,6-dichlorophenyl)acetamide	-131.828	-112.474	-4.89019	5	-6.73357	23	350.219
3000870	Trovirdine	1-(5-bromopyridin-2-yl)-3-(2-pyridin-2-ylethyl)thiourea	-131.639	-113.262	-5.96118	4	0	19	335.222
441300	abacavir	[(1S,4R)-4-[2-amino-6-(cyclopropylamino)purin-9-yl]cyclopent-2-en-1-yl]methanol	-129.468	-132.802	-6.3239	4	-8.80073	21	285.324

Continued Table 1.									
60613	Cidofovir	[(2S)-1-(4-amino-2-oxopyrimidin-1-yl)-3-hydroxypropan-2-yl]oxymethylphosphonic acid	-129.468	-108.259	-6.01438	6	-6.86134	18	277.171
118214142	Tenofovir amibufenamide	propan-2-yl 2-[[[(2R)-1-(6-aminopurin-9-yl)propan-2-yl]oxymethylphenoxyphosphoryl]amino]-2-methylpropanoate	-128.599	-134.772	-3.96389	12	-0.12526	34	490.493
16739244	Lersivirine	5-[3,5-diethyl-1-(2-hydroxyethyl)pyrazol-4-yl]oxybenzene-1,3-dicarbonitrile	-127.386	-125.632	-5.46226	8	-1.41921	23	310.35
3000323	Tivirapine	(11S)-7-chloro-11-methyl-10-(3-methylbut-2-enyl)-1,3,10-triazatricyclo[6.4.1.04,13]trideca-4(13),5,7-triene-2-thione	-123.985	-123.284	-5.87065	2	-1.91654	21	320.86
6483431	Islatravir	(2R,3S,5R)-5-(6-amino-2-fluoropurin-9-yl)-2-ethynyl-2-(hydroxymethyl)oxolan-3-ol	-123.968	-119.153	-5.67397	3	-8.869	21	292.246
55281	NETIVU-DINE	1-[(2R,3S,4S,5R)-3,4-dihydroxy-5-(hydroxymethyl)oxolan-2-yl]-5-prop-1-ynylpyrimidine-2,4-dione	-122.617	-116.404	-5.82019	4	-8.4128	20	282.249
135398513	acyclovir	2-amino-9-(2-hydroxyethoxymethyl)-1H-purin-6-one	-122.169	-120.996	-7.56223	4	-9.13901	16	225.205
35370	zidovudine	1-[(2R,4S,5S)-4-azido-5-(hydroxymethyl)oxolan-2-yl]-5-methylpyrimidine-2,4-dione	-121.126	-112.122	-5.90115	3	-10.0391	19	268.249
72180	Lodenosine	[(2S,4S,5R)-5-(6-aminopurin-9-yl)-4-fluorooxolan-2-yl]methanol	-121.043	-114.348	-6.35269	2	-7.79013	18	253.233
135398739	Didanosine	9-[(2R,5S)-5-(hydroxymethyl)oxolan-2-yl]-1H-purin-6-one	-120.026	-114.143	-6.71428	2	-8.63011	17	236.227
18283	stavudine	1-[(2R,5S)-5-(hydroxymethyl)-2,5-dihydrofuran-2-yl]-5-methylpyrimidine-2,4-dione	-120.003	-116.549	-7.28428	2	-7.31295	16	224.213
135433604	Carbovir	2-amino-9-[(1R,4S)-4-(hydroxymethyl)cyclopent-2-en-1-yl]-1H-purin-6-one	-119.894	-118.514	-6.5841	2	-5.39359	18	247.253
154048	Opaviraline	propan-2-yl (2S)-2-ethyl-7-fluoro-3-oxo-2,4-dihydroquinoxaline-1-carboxylate	-119.55	-112.526	-5.62631	4	-6.73452	20	280.295

Continued Table 1.

446727	Brivudine	5-[(E)-2-bromoethenyl]-1-[(2R,4S,5R)-4-hydroxy-5-(hydroxymethyl)oxolan-2-yl]pyrimidine-2,4-dione	-119.344	-104.315	-5.49029	3	-5.81182	19	333.135
135398748	penciclovir	2-amino-9-[4-hydroxy-3-(hydroxymethyl)butyl]-1H-purin-6-one	-119.23	-110.518	-6.13988	5	-6.16508	18	253.258
135398740	ganciclovir	2-amino-9-(1,3-dihydroxypropan-2-yloxymethyl)-1H-purin-6-one	-119.056	-113.134	-6.2852	5	-8.91961	18	255.231
55262	Navuridine	1-[(2R,4S,5S)-4-azido-5-(hydroxymethyl)oxolan-2-yl]pyrimidine-2,4-dione	-118.994	-108.73	-6.04053	3	-6.37911	18	254.223
21704	Vidarabine	(2R,3S,4S,5R)-2-(6-aminopurin-9-yl)-5-(hydroxymethyl)oxolane-3,4-diol	-118.535	-127.01	-6.68475	2	-7.9224	19	267.241
64139	efavirenz	(4S)-6-chloro-4-(2-cyclopropylethynyl)-4-(trifluoromethyl)-1H-3,1-benzoxazin-2-one	-116.809	-104.584	-4.9802	4	0	21	314.667
135431817	Lagociclovir	2-amino-9-[(2R,4S,5R)-4-fluoro-5-(hydroxymethyl)oxolan-2-yl]-1H-purin-6-one	-116.513	-110.604	-5.82127	2	-2.5	19	269.232
4463	nevirapine	2-cyclopropyl-7-methyl-2,4,9,15-tetraza-tricyclo[9.4.0.0.3,8]pentadeca-1(11),3,5,7,12,14-hexaen-10-one	-116.221	-102.557	-5.12785	1	-1.68958	20	266.298
455041	Apricitabine	4-amino-1-[(2R,4R)-2-(hydroxymethyl)-1,3-oxathiolan-4-yl]pyrimidin-2-one	-114.693	-105.654	-7.04361	2	-8.05436	15	229.256
64973	Dexelvucitabine	4-amino-5-fluoro-1-[(2R,5S)-5-(hydroxymethyl)-2,5-dihydrofuran-2-yl]pyrimidin-2-one	-114.425	-105.953	-6.62204	2	-9.26732	16	227.192
469717	Elvucitabine	4-amino-5-fluoro-1-[(2S,5R)-5-(hydroxymethyl)-2,5-dihydrofuran-2-yl]pyrimidin-2-one	-113.858	-101.017	-6.31358	2	-7.42511	16	227.192
3008897	Censavudine	1-[(2R,5R)-5-ethynyl-5-(hydroxymethyl)-2H-furan-2-yl]-5-methylpyrimidine-2,4-dione	-113.232	-99.6344	-5.53524	3	-8.30063	18	247.227
20039	2',3'-Dideoxyadenosine;	[(2S,5R)-5-(6-aminopurin-9-yl)oxolan-2-yl]methanol	-113.032	-118.68	-6.98119	2	-4.75246	17	235.243

Continued Table 1.

3885	beta-Lapachone	2,2-dimethyl-3,4-dihydrobenzo[h]chromene-5,6-dione	-112.898	-94.1763	-5.23202	0	0	18	242.27
451480	Raluridine	5-chloro-1-[(2R,4S,5R)-4-fluoro-5-(hydroxymethyl)oxolan-2-yl]pyrimidine-2,4-dione	-112.657	-103.349	-6.07935	2	-7.25271	17	264.638
73115	Clevudine	1-[(2S,3R,4S,5S)-3-fluoro-4-hydroxy-5-(hydroxymethyl)oxolan-2-yl]-5-methylpyrimidine-2,4-dione	-112.291	-99.9118	-5.55065	2	-7.02089	18	260.219
124088	Amdoxovir	[(2R,4R)-4-(2,6-diaminopurine-9-yl)-1,3-dioxolan-2-yl]methanol	-111.527	-117.572	-6.53181	2	-5.06086	18	252.23
33039	Alovudine;	1-[(2R,4S,5R)-4-fluoro-5-(hydroxymethyl)oxolan-2-yl]-5-methylpyrimidine-2,4-dione	-111.046	-100.413	-5.90663	2	-5.1703	17	244.22
159269	Telbivudine	1-[(2S,4R,5S)-4-hydroxy-5-(hydroxymethyl)oxolan-2-yl]-5-methylpyrimidine-2,4-dione	-108.424	-102.016	-6.00093	2	-5.66207	17	242.229
60825	Lamivudine	4-amino-1-[(2R,5S)-2-(hydroxymethyl)-1,3-oxathiolan-5-yl]pyrimidin-2-one	-105.183	-101.227	-6.74845	2	-6.87127	15	229.256
60877	Emtricitabine	4-amino-5-fluoro-1-[(2R,5S)-2-(hydroxymethyl)-1,3-oxathiolan-5-yl]pyrimidin-2-one	-104.215	-92.3249	-5.77031	2	-5.29629	16	247.247
47318	Oltipraz	4-methyl-5-pyrazin-2-yl-dithiole-3-thione	-103.877	-93.3068	-7.17744	1	0	13	226.342
3415	foscarnet	phosphonoformic acid	-103.713	-87.2466	-12.4638	1	-6.4567	7	122.981
3414	Foscavir	Phosphonatoformate	-103.218	-79.0771	-11.2967	1	-9.22998	7	122.981
546	Phosphonoacetic acid	Phosphonoacetic acid	-102.804	-94.182	-11.7728	2	-8.80605	8	137.008

digestive absorption, but some compounds, such as 9574768, 135398742, 11599486, 135413535, 1783, 60871, 73505111, 464205, 60172, 60613, 118214142, 55281, 135398748, 135398740, 21704, and 124088, have poor digestive absorption.

On the other hand, a list of compounds with different CIDs numbers, 60848, 65013, 3963, 3000323, 154048, 64139, 4463, and 3885, have the ability to cross the blood-brain barrier. This means they can pass through the protective layer surrounding the brain and access the central nervous system, potentially impacting brain function

and overall health.

However, there is another group of compounds with CIDs numbers 5625, 9574768, 60848, 135398742, 44603336, 135413535, 3324, 60871, 441300, 118214142, 64139, and 4463 that are known substrates of the Pgp (P-glycoprotein) protein. Pgp is a transmembrane protein that plays a crucial role in cellular defense by actively transporting these substances out of the cell, preventing their accumulation and maintaining homeostasis within the cellular environment. This characteristic may affect the efficacy of certain drugs and therapeutic agents, as well as the way these com-

16739244	118214142	60613	441300	3000870	3963	135398508	65013	3000493	3000926	60172	464205	73505111	60871	6451164
310.35	490.49	279.19	286.33	337.24	351.23	277.28	302.37	340.46	335.85	273.19	287.21	491.73	501.47	366.42
23	34	18	21	19	23	20	22	22	22	18	19	33	34	28
11	15	6	9	12	12	9	12	6	11	9	9	18	9	18
0.35	0.45	0.5	0.5	0.15	0.18	0.42	0.41	0.47	0.24	0.38	0.44	0.17	0.65	0.09
6	12	6	4	6	5	2	6	6	6	5	5	6	15	5
5	9	7	4	2	2	5	3	3	2	7	7	12	11	4
1	2	4	3	2	2	4	1	1	1	3	3	1	1	2
84.95	128.95	61.82	80.4	83.73	93.13	72.39	87.32	101.29	95.51	62.68	67.48	98.91	122.26	110.41
94.86	153.29	157.71	101.88	81.93	72.19	130.05	64.09	108.19	66.49	146.19	146.19	113.66	176.79	97.42
2.58	3.71	-0.6	2.12	2.6	2.39	0.79	2.55	3.34	3.4	-0.09	0.41	2.28	3.72	3.09
2.11	2.11	-3.61	0.87	2.4	4.4	-1.12	2.59	2.72	4.92	-2.03	-1.6	2.75	1.82	4.55
27.60%	8.83%	199000.00%	-	10.30%	0.50%	2450.00%	13.40%	11.50%	0.34%	13900.00%	6680.00%	1.16%	25.00%	0.28%
0.09%	0.02%	712.00%	0.61%	0.03%	0.00%	8.82%	0.04%	0.03%	0.00%	50.70%	23.30%	0.00%	0.05%	0.00%
Soluble	Soluble	Highly soluble	Soluble	Soluble	Moderately soluble	Very soluble	Soluble	Soluble	Moderately soluble	Very soluble	Very soluble	Moderately soluble	Soluble	Moderately soluble

21704	55262	135398740	135398748	446727	154048	135433604	18283	135398739	72180	35370	135398513	55281	6483431	3000323
267.24	253.21	255.23	253.26	333.14	280.29	247.25	224.21	236.23	253.23	267.24	225.2	282.25	293.25	321.87
19	18	18	18	19	20	18	16	17	18	19	16	20	21	21
9	6	9	9	6	6	9	6	9	9	6	9	6	9	9
0.5	0.56	0.44	0.5	0.45	0.43	0.36	0.4	0.5	0.5	0.6	0.38	0.5	0.42	0.44
2	3	5	5	3	4	2	2	2	2	3	4	2	2	2
7	7	6	5	5	4	4	4	5	6	7	5	6	7	1
4	2	4	4	3	1	3	2	2	2	2	3	4	3	1
62.67	56.77	61.64	65.37	71.07	79.58	66.42	56.44	58.77	60.4	61.73	55.68	67.01	69.28	96.23
139.54	134.07	139.28	130.05	104.55	58.64	109.82	84.32	93.03	99.08	134.07	119.05	124.78	119.31	56.05
0.71	1.37	0.16	0.48	1.29	2.75	0.7	1.67	0.88	1.31	1.76	0.48	1.43	1.51	3.28
-1.05	-0.32	-1.66	-1.58	-0.42	2.49	-0.58	-0.81	-1.47	-0.14	0.05	-1.56	-1.94	-0.59	3.52
2360.00%	1400.00%	9780.00%	8890.00%	702.00%	22.00%	1400.00%	3060.00%	5430.00%	698.00%	729.00%	8850.00%	9840.00%	990.00%	1.86%
8.83%	5.53%	38.30%	35.10%	2.11%	0.08%	5.68%	13.60%	23.00%	2.76%	2.73%	39.30%	34.90%	3.38%	0.01%
Very soluble	Very soluble	Very soluble	Very soluble	Very soluble	Soluble	Very soluble	Very soluble	Very soluble	Very soluble	Very soluble	Very soluble	Very soluble	Very soluble	Moderately soluble

546	3414	47318	60877	60825	159269	33039	124088	73115	451480	3885	20039	3008897	469717	64973	455041	4463	64139
140.03	122.98	226.34	247.25	229.26	242.23	244.22	252.23	260.22	264.64	242.27	235.24	248.23	227.19	227.19	229.26	266.3	315.67
8	7	13	16	15	17	17	18	18	17	18	17	18	16	16	15	20	21
0	0	11	6	6	6	6	9	6	6	6	9	6	6	6	6	15	6
0.5	0	0.12	0.5	0.5	0.6	0.6	0.44	0.6	0.56	0.33	0.5	0.33	0.33	0.33	0.5	0.27	0.36
2	1	1	2	2	2	2	2	2	2	0	2	2	2	2	2	1	1
5	5	2	5	4	5	5	6	6	5	3	5	4	5	5	4	3	5
3	0	0	2	2	3	2	3	3	2	0	2	2	2	2	2	1	1
24.49	15.06	59.02	56.27	56.31	58.07	56.96	61.03	58.12	57.01	67.86	60.35	64.25	53.01	53.01	56.31	78.2	73.18
104.64	113.13	114.35	115.67	115.67	104.55	84.32	134.33	104.55	84.32	43.37	99.08	84.32	90.37	90.37	115.67	63.57	38.33
-0.79	-1.02	1.88	1.2	0.97	1.25	1.51	1.23	1.29	1.15	2.23	1.39	1.46	1.31	1.31	1.06	2.42	2.68
-2.01	-1.74	1.07	-0.62	-0.93	-1.17	-0.28	-1.22	-0.86	-0.17	2.2	-0.22	-0.71	-1.26	-1.26	-1.2	1.96	4.01
68600.00%	44600.00%	75.40%	1840.00%	3320.00%	4470.00%	1200.00%	3380.00%	2450.00%	831.00%	25.70%	895.00%	2230.00%	5700.00%	5700.00%	4910.00%	16.20%	1.07%
490.00%	363.00%	0.33%	7.45%	14.50%	18.50%	4.93%	13.40%	9.41%	3.14%	0.11%	3.80%	8.99%	25.10%	25.10%	21.40%	0.06%	0.00%
Highly soluble	Highly soluble	Soluble	Very soluble	Very soluble	Very soluble	Very soluble	Very soluble	Very soluble	Very soluble	Soluble	Very soluble	Very soluble	Very soluble	Very soluble	Very soluble	Soluble	Moderately soluble

pounds interact with other substances within the body.

The compounds with CIDs numbers 135398742, 135413535, 3324, 464205, 60172,

65013, 135398508, 60613, 6483431, 55281, 135398513, 35370, 72180, 135398739, 18283, 135433604, 446727, 135398748, 135398740, 55262, 21704, 455041, 64973, 469717, 3008897, 20039, 451480, 73115, 124088, 33039, 159269, 60825, 60877, 3414, and 546 do not inhibit any of the cytochrome P450 enzymes.

Furthermore, the skin absorption rates vary among these compounds. The ligands with CIDs numbers 3000926 and 214347 show the highest skin permeability rates among the studied compounds, as they can penetrate the skin. However, compounds with CIDs numbers 193962,

1783, 6451164, 3963, 3000323, and 64139 exhibit weaker skin absorption. This information can be valuable for understanding the potential applications, effects, and interactions of these compounds with various drugs.

4. Discussion

The HIV-1 Reverse Transcriptase (RT) consists of p66 and p51 subunits. These subunits are derived from the Gag-Pol polyprotein, which is cleaved by the viral protease. The p66 subunit contains the active sites for DNA polymerase and

Table 1. Pharmaceutical Properties of studied compounds.

CID Number	GI absorption	BBB permeant	Pgp substrate	CYP1A2 inhibitor	CYP2C19 inhibitor	CYP2C9 inhibitor	CYP2D6 inhibitor	CYP3A4 inhibitor	log Kp (cm/s)
5625	High	No	Yes	No	No	Yes	Yes	Yes	-7.35
9574768	Low	No	Yes	No	Yes	No	No	Yes	-7.84
60848	High	Yes	Yes	Yes	No	Yes	Yes	Yes	-6.47
214347	High	No	No	Yes	Yes	Yes	Yes	Yes	-4.92
193962	Low	No	No	Yes	Yes	Yes	No	Yes	-5.8
135398742	Low	No	Yes	No	No	No	No	No	-8.71
11599486	Low	No	No	No	Yes	Yes	No	No	-6.57
44603336	Low	No	Yes	No	No	No	No	Yes	-8.4
135413535	Low	No	Yes	No	No	No	No	No	-8.91
58460047	High	No	No	No	No	Yes	No	No	-7.41
1783	Low	No	No	No	Yes	Yes	No	Yes	-5.85
3324	High	No	Yes	No	No	No	No	No	-8.3
6451164	High	No	No	Yes	Yes	Yes	No	Yes	-5.3
60871	Low	No	Yes	Yes	Yes	No	No	Yes	-8.07
73505111	Low	No	No	Yes	No	Yes	No	No	-7.35
464205	Low	No	No	No	No	No	No	No	-9.19
60172	Low	No	No	No	No	No	No	No	-9.41
3000926	High	No	No	Yes	Yes	Yes	Yes	Yes	-4.86
3000493	High	No	No	Yes	Yes	Yes	No	No	-6.45
65013	High	Yes	No	No	No	No	No	No	-6.31
135398508	High	No	No	No	No	No	No	No	-8.79
3963	High	Yes	No	Yes	Yes	Yes	Yes	Yes	-5.32
3000870	High	No	No	Yes	Yes	Yes	Yes	Yes	-6.65
441300	High	No	Yes	Yes	No	No	No	No	-7.43
60613	Low	No	No	No	No	No	No	No	-10.57
118214142	Low	No	Yes	No	Yes	No	No	Yes	-7.79
16739244	High	No	No	Yes	No	Yes	No	Yes	-6.7
3000323	High	Yes	No	Yes	Yes	Yes	No	Yes	-5.76
6483431	High	No	No	No	No	No	No	No	-8.51
55281	Low	No	No	No	No	No	No	No	-9.4
135398513	High	No	No	No	No	No	No	No	-8.78

Continued Table 3.

35370	High	No	No	No	No	No	No	No	-7.89
72180	High	No	No	No	No	No	No	No	-7.94
135398739	High	No	No	No	No	No	No	No	-8.78
18283	High	No	No	No	No	No	No	No	-8.24
135433604	High	No	No	No	No	No	No	No	-8.22
154048	High	Yes	No	No	Yes	No	No	No	-6.24
446727	High	No	No	No	No	No	No	No	-8.63
135398748	Low	No	No	No	No	No	No	No	-8.97
135398740	Low	No	No	No	No	No	No	No	-9.04
55262	High	No	No	No	No	No	No	No	-8.07
21704	Low	No	No	No	No	No	No	No	-8.68
64139	High	Yes	Yes	Yes	Yes	Yes	No	No	-5.38
4463	High	Yes	Yes	Yes	No	No	No	No	-6.53
455041	High	No	No	No	No	No	No	No	-8.55
64973	High	No	No	No	No	No	No	No	-8.58
469717	High	No	No	No	No	No	No	No	-8.58
3008897	High	No	No	No	No	No	No	No	-8.32
20039	High	No	No	No	No	No	No	No	-7.89
3885	High	Yes	No	Yes	Yes	No	No	No	-6.22
451480	High	No	No	No	No	No	No	No	-8.03
73115	High	No	No	No	No	No	No	No	-8.5
124088	Low	No	No	No	No	No	No	No	-8.7
33039	High	No	No	No	No	No	No	No	-7.99
159269	High	No	No	No	No	No	No	No	-8.61
60825	High	No	No	No	No	No	No	No	-8.36
60877	High	No	No	No	No	No	No	No	-8.25
47318	High	No	No	Yes	No	No	No	No	-6.92
3414	High	No	No	No	No	No	No	No	-8.29
546	High	No	No	No	No	No	No	No	-8.58

RNase H activities, while p51 serves a structural role. The polymerase domain of p66 comprises four subdomains: fingers, palm, thumb, and connection. The p51 subunit shares the same structural features as p66's polymerase domain but with distinct positions of these subdomains. These enzymatic functions are essential for converting the viral RNA genome into double-stranded DNA, which is then integrated into the host genome by the Integrase enzyme. The nucleic-acid binding cleft in HIV-1 RT is primarily formed by subdomains from both p66 and p51, allowing the nucleic acid to interact with both the polymerase and RNase H active sites. The α H and α I helices of the p66 thumb play a crucial role in positioning the nucleic acid by interacting with both the primer and template strands. The "DNA primer grip" is

a conserved structural motif that helps position the 3'-OH end of the primer strand at the polymerase active site. Alterations in the primer grip can lead to disruptions in nucleic acid binding, potentially affecting the overall functionality of the polymerase and RNase H activities within the RT enzyme. In the polymerase active site of p66, the palm subdomain contains three catalytic carboxylates (D110, D185, and D186) that bind two divalent ions, primarily Mg^{2+} *in vivo* and Mn^{2+} *in vitro*, for catalysis (28, 29).

Non-nucleoside reverse transcriptase inhibitors (NNRTIs) are a class of antiretroviral drugs that inhibit HIV replication. They function by binding to the non-nucleoside reverse transcriptase inhibitor-binding pocket (NNIBP), a hydrophobic region adjacent to the polymerase ac-

tive site, approximately 10 Å away. The NNIBP comprises amino acid residues from both p66 and p51 subunits of RT, including L100, K101, K103, V106, T107, V108, V179, Y181, Y188, V189, G190, F227, W229, L234, and Y318 from p66, and E138 from p51 (29).

Understanding the pharmacological properties of NNRTIs and NRTIs medicinal compounds is crucial for utilizing the appropriate pharmaceutical form and maximizing the effectiveness of these medicinal compounds. This study investigated the binding affinity and binding site of 62 reverse transcriptase inhibitor compounds. An interesting finding was that these drugs show a higher binding affinity for the P51 subunit. However, some compounds, such as those with CID Numbers 60871, 455041, and 47318, exhibited a greater binding affinity for the larger P66 subunit. Additionally, certain compounds bound to the site between the two subunits and demonstrated a higher binding affinity for the reverse transcriptase enzyme model compared to other compounds studied. Previous research has suggested point mutations in the subunits of the reverse transcriptase enzyme.

HIV-1, the virus responsible for Acquired Immunodeficiency Syndrome (AIDS), has developed various resistance mechanisms to combat antiretroviral drugs, particularly Non-Nucleoside Reverse Transcriptase Inhibitors (NNRTIs). These resistance mechanisms enable the virus to continue replicating and evade the effects of the treatment. Two primary resistance mechanisms include exclusion and excision. Exclusion resistance is characterized by enhanced discrimination of nucleoside reverse transcriptase inhibitors (NRTIs), as seen in M184V/I mutations. These mutations make it challenging for NRTIs to effectively inhibit the reverse transcriptase enzyme, allowing the virus to continue replicating. Excision resistance occurs after the incorporation of NRTIs into viral DNA. This resistance is demonstrated by AZT resistance and associated mutations like M41L, D67N, K70R, L210W, T215F/Y, and K219E/Q. These mutations enable the virus to remove the incorporated NRTIs from its DNA, allowing replication to continue. Other exclusion mutations, such as L74V, K65R, and Q151M, affect the fingers or palm region of the reverse transcriptase enzyme,

potentially altering deoxynucleotide triphosphate (dNTP) binding and impacting the overall efficiency of the enzyme. Specific mutations, like T215F/Y, can enhance ATP binding in AZT-resistant reverse transcriptase enzymes, enabling HIV-1 to maintain its replication capacity despite the presence of NRTIs. AZT-resistant reverse transcriptases can acquire additional "fingers insertion" mutations, which broaden the set of NRTIs they can excise from the viral DNA (30, 31).

These mutations are located near position 69 of the fingers subdomain of HIV-1 reverse transcriptase. Mutations associated with Lamivudine (3TC) / emtricitabine (FTC) resistance, such as M184V/I, reduce excision efficiency. The connection subdomain mutation N348I confers moderate cross-resistance to both NRTIs and NNRTIs. NNRTI drugs, including nevirapine, delavirdine, efaviriz, etravirine, and several potent NNRTIs in clinical trials, are used to treat HIV-1 infections. Common NNRTI resistance mutations include K103N and Y181C (30-32).

5. Conclusion

The HIV-1 Reverse Transcriptase (RT) enzyme is crucial for converting the viral RNA genome into double-stranded DNA. This enzyme consists of p66 and p51 subunits, each with distinct structural features and roles in the enzyme's function. Non-nucleoside reverse transcriptase inhibitors (NNRTIs) are a class of antiretroviral drugs that inhibit HIV replication by binding to the non-nucleoside reverse transcriptase inhibitor-binding pocket (NNIBP) near the polymerase active site. Understanding the pharmacological properties of NNRTIs and NRTIs medicinal compounds is essential for optimizing their effectiveness in managing HIV-1 infections. The study mentioned investigates the binding affinity and site of 62 reverse transcriptase inhibitor compounds, showing their highest affinity for this enzyme.

Acknowledgment

We would like to thank the Behbahan Faculty of Medical Science for their support.

Conflict of Interest

The authors declare no conflict of interest.

References

1. Payagala S, Pozniak A. The global burden of HIV. *Clin Dermatol*. 2024 Mar-Apr;42(2):119-127. doi: 10.1016/j.clindermatol.2024.02.001. Epub 2024 Feb 21. PMID: 38387533..
2. Panwar U, Chandra I, Selvaraj C, Singh SK. Current Computational Approaches for the Development of Anti-HIV Inhibitors: An Overview. *Curr Pharm Des*. 2019;25(31):3390-3405. doi: 10.2174/1381612825666190911160244. PMID: 31538884.
3. Jonckheere H, Anné J, De Clercq E. The HIV-1 reverse transcription (RT) process as target for RT inhibitors. *Med Res Rev*. 2000 Mar;20(2):129-54. doi: 10.1002/(sici)1098-1128(200003)20:2<129::aid-med2>3.0.co;2-a. PMID: 10723025.
4. Hu WS, Hughes SH. HIV-1 reverse transcription. *Cold Spring Harb Perspect Med*. 2012 Oct 1;2(10):a006882. doi: 10.1101/cshperspect.a006882. PMID: 23028129; PMCID: PMC3475395.
5. Jochmans D. Novel HIV-1 reverse transcriptase inhibitors. *Virus Res*. 2008 Jun;134(1-2):171-85. doi: 10.1016/j.virusres.2008.01.003. Epub 2008 Mar 4. PMID: 18308412.
6. Sarafianos SG, Marchand B, Das K, Himmel DM, Parniak MA, Hughes SH, Arnold E. Structure and function of HIV-1 reverse transcriptase: molecular mechanisms of polymerization and inhibition. *J Mol Biol*. 2009 Jan 23;385(3):693-713. doi: 10.1016/j.jmb.2008.10.071. Epub 2008 Nov 3. PMID: 19022262; PMCID: PMC2881421.
7. Tachedjian G, Radzio J, Sluis-Cremer N. Relationship between enzyme activity and dimeric structure of recombinant HIV-1 reverse transcriptase. *Proteins*. 2005;60(1):5-13.
8. Chiu TK, Davies DR. Structure and function of HIV-1 integrase. *Curr Top Med Chem*. 2004;4(9):965-77. doi: 10.2174/1568026043388547. PMID: 15134551.
9. Himmel DM, Maegley KA, Pauly TA, Bauman JD, Das K, Dharia C, Clark AD Jr, Ryan K, Hickey MJ, Love RA, Hughes SH, Bergqvist S, Arnold E. Structure of HIV-1 reverse transcriptase with the inhibitor beta-Thujaplicinol bound at the RNase H active site. *Structure*. 2009 Dec 9;17(12):1625-1635. doi: 10.1016/j.str.2009.09.016. PMID: 20004166; PMCID: PMC3365588.
10. Esposito F, Corona A, Tramontano E. HIV-1 Reverse Transcriptase Still Remains a New Drug Target: Structure, Function, Classical Inhibitors, and New Inhibitors with Innovative Mechanisms of Actions. *Mol Biol Int*. 2012;2012:586401. doi: 10.1155/2012/586401. Epub 2012 Jun 20. PMID: 22778958; PMCID: PMC3388302.
11. Gu SX, Zhu YY, Wang C, Wang HF, Liu GY, Cao S, Huang L. Recent discoveries in HIV-1 reverse transcriptase inhibitors. *Curr Opin Pharmacol*. 2020 Oct;54:166-172. doi: 10.1016/j.coph.2020.09.017. Epub 2020 Nov 8. PMID: 33176248.
12. El Safadi Y, Vivet-Boudou V, Marquet R. HIV-1 reverse transcriptase inhibitors. *Appl Microbiol Biotechnol*. 2007 Jun;75(4):723-37. doi: 10.1007/s00253-007-0919-7. Epub 2007 Mar 17. PMID: 17370068.
13. Spence RA, Kati WM, Anderson KS, Johnson KA. Mechanism of inhibition of HIV-1 reverse transcriptase by nonnucleoside inhibitors. *Science*. 1995 Feb 17;267(5200):988-93. doi: 10.1126/science.7532321. PMID: 7532321; PMCID: PMC7526747.
14. De Clercq E. Non-nucleoside reverse transcriptase inhibitors (NNRTIs): past, present, and future. *Chem Biodivers*. 2004 Jan;1(1):44-64. doi: 10.1002/cbdv.200490012. PMID: 17191775.
15. De Clercq E. The role of non-nucleoside reverse transcriptase inhibitors (NNRTIs) in the therapy of HIV-1 infection. *Antiviral Res*. 1998 Jun;38(3):153-79. doi: 10.1016/s0166-3542(98)00025-4. PMID: 9754886.
16. Wang Y, De Clercq E, Li G. Current and emerging non-nucleoside reverse transcriptase inhibitors (NNRTIs) for HIV-1 treatment. *Expert Opin Drug Metab Toxicol*. 2019 Oct;15(10):813-829. doi: 10.1080/17425255.2019.1673367. Epub 2019 Oct 17. PMID: 31556749.
17. Namasivayam V, Vanangamudi M, Kramer VG, Kurup S, Zhan P, Liu X, Kongsted J, Byrareddy SN. The Journey of HIV-1 Non-Nucleoside Reverse Transcriptase Inhibitors (NNRTIs) from Lab to Clinic. *J Med Chem*. 2019 May 23;62(10):4851-4883. doi: 10.1021/acs.jmedchem.8b00843. Epub 2018 Dec 27. PMID: 30516990; PMCID: PMC7049092.
18. Zhuang C, Pannecouque C, De Clercq E, Chen F. Development of non-nucleoside reverse

transcriptase inhibitors (NNRTIs): our past twenty years. *Acta Pharm Sin B*. 2020 Jun;10(6):961-978. doi: 10.1016/j.apsb.2019.11.010. Epub 2019 Nov 21. PMID: 32642405; PMCID: PMC7332669.

19. Das K, Martinez SE, Arnold E. Structural Insights into HIV Reverse Transcriptase Mutations Q151M and Q151M Complex That Confer Multinucleoside Drug Resistance. *Antimicrob Agents Chemother*. 2017 May 24;61(6):e00224-17. doi: 10.1128/AAC.00224-17. PMID: 28396546; PMCID: PMC5444136

20. Kim S, Thiessen PA, Bolton EE, Chen J, Fu G, Gindulyte A, Han L, He J, He S, Shoemaker BA, Wang J, Yu B, Zhang J, Bryant SH. PubChem Substance and Compound databases. *Nucleic Acids Res*. 2016 Jan 4;44(D1):D1202-13. doi: 10.1093/nar/gkv951. Epub 2015 Sep 22. PMID: 26400175; PMCID: PMC4702940.

21. Bitencourt-Ferreira G, de Azevedo WF Jr. Molegro Virtual Docker for Docking. *Methods Mol Biol*. 2019;2053:149-167. doi: 10.1007/978-1-4939-9752-7_10. PMID: 31452104.

22. Daina A, Michielin O, Zoete V. SwissADME: a free web tool to evaluate pharmacokinetics, drug-likeness and medicinal chemistry friendliness of small molecules. *Sci Rep*. 2017 Mar 3;7:42717. doi: 10.1038/srep42717. PMID: 28256516; PMCID: PMC5335600.

23. Daina A, Michielin O, Zoete V. iLOGP: a simple, robust, and efficient description of n-octanol/water partition coefficient for drug design using the GB/SA approach. *J Chem Inf Model*. 2014 Dec 22;54(12):3284-301. doi: 10.1021/ci500467k. Epub 2014 Nov 25. PMID: 25382374.

24. Daina, A., & Zoete, V. (2016). A boiled-egg to predict gastrointestinal absorption and brain penetration of small molecules. *ChemMedChem*, 11(11), 1117-1121

25. Yousefi, R. Molecular Docking Study of Rosmarinic Acid and Its Analog Compounds on Sickle Cell Hemoglobin. *Eurasian J Sci Technol*.2024;4(4):303-330. doi: 10.48309/

ejst.2024.444334.1130]

26. Yousefi R. The Potential Application of Roselle Extracts (*Hibiscus sabdariffa* L.) in Managing Diabetes Mellitus. *J Adv Pharm Res*. 2024; 8(2):38-48. doi: 10.21608/aprh.2024.277267.1260

27. Yousefi R. Binding of curcumin near the GBT440 binding site at the alpha cleft in the sickle cell hemoglobin model [Pdb ID: 1NEJ]. *J Adv Biomed & Pharm Sci*.2024;7(2):70-74.

28. Powell MD, Beard WA, Bebenek K, Howard KJ, Le Grice SF, Darden TA, Kunkel TA, Wilson SH, Levin JG. Residues in the alphaH and alphaI helices of the HIV-1 reverse transcriptase thumb subdomain required for the specificity of RNase H-catalyzed removal of the polypurine tract primer. *J Biol Chem*. 1999 Jul 9;274(28):19885-93. doi: 10.1074/jbc.274.28.19885. PMID: 10391934.

29. Titmuss SJ, Keller PA, Griffith R. Docking experiments in the flexible non-nucleoside inhibitor binding pocket of HIV-1 reverse transcriptase. *Bioorg Med Chem*. 1999 Jun;7(6):1163-70. doi: 10.1016/s0968-0896(99)00012-7. PMID: 10428388.

30. Svarovskaia ES, Cheslock SR, Zhang WH, Hu WS, Pathak VK. Retroviral mutation rates and reverse transcriptase fidelity. *Front Biosci*. 2003 Jan 1;8:d117-34. doi: 10.2741/957. PMID: 12456349.

31. Shafer RW, Rhee SY, Pillay D, Miller V, Sandstrom P, Schapiro JM, Kuritzkes DR, Bennett D. HIV-1 protease and reverse transcriptase mutations for drug resistance surveillance. *AIDS*. 2007 Jan 11;21(2):215-23. doi: 10.1097/QAD.0b013e328011e691. PMID: 17197813; PMCID: PMC2573394.

32. Kellam P, Boucher CA, Larder BA. Fifth mutation in human immunodeficiency virus type 1 reverse transcriptase contributes to the development of high-level resistance to zidovudine. *Proc Natl Acad Sci U S A*. 1992 Mar 1;89(5):1934-8. doi: 10.1073/pnas.89.5.1934. PMID: 1371886; PMCID: PMC48568.

